

Petrology, geochemistry and structure of the Pissila batholith and the Saaba Zone gneiss



Honour Project First Draft: By Nosizwe Simoko (309922)

Supervisors Profs. Kerstin Saalman and Kim Ncube-Hein.

TABLE OF CONTENT

Abstract.....	1
1. Introduction.....	2
2. Regional Geology.....	3
2.1. Archean domain.....	3
2.2. Palaeoproterozoic/Stratigraphy.....	4
2.3. Magmatic intrusions.....	5
2.4. Regional Tectonics.....	5
3. Aim	7
4. Methodology.....	8
5. Petrography.....	10
5.1. Granodiorite.....	10
5.2. Gneiss.....	11
5.3. Migmatites.....	12
6. Geochemistry	16
6.1. Major Elements.....	16
6.2. Trace Elements.....	23
7. Discussion.....	26
7.1. Comparison between the gneiss and the granodiorite.....	26
7.2. Gneiss and migmatite.....	26
7.3. Granodiorite.....	27
Deformation.....	28
8. Conclusion.....	32

Acknowledgment33
Appendix.....34
Reference.....35

Abstract

The Pissila batholith is a foliated coarse-grained granodiorite, which is located in north eastern Burkina Faso. The batholith was emplaced at 2143 ± 12 Ma and 2117 ± 17 Ma, coeval with the Eburnean orogeny. The Eburnean orogeny represents a period of major crustal growth in an island arc setting. The batholith is geochemically similar to other calc-alkaline granitoids in the domain. The Saaba zone gneiss, which is locally migmatitic is located within the Pissila batholith. Geochemically, the gneiss and migmatites have some Archean TTG affiliations. Granitoids that are associated with gneisses and migmatites were previously described in north eastern Burkina Faso, Côte d'Ivoire and Senegal. These studies concluded that the granitoids intruded into the pre-existing gneissic terrane. This study suggests that the Saaba zone and Pissila batholith are geochemically and petrological different from each other. The Saaba zone gneiss does not represent a deformed region of the Pissila batholith. Based on similarities of the study area to other granitoid-gneissic terrane, the Saaba zone may predate the Pissila batholith. It is also proposed that the gneiss preserve an older deformation event D1, which lead to amphibolite facies metamorphism. The second deformation D2 affected both granodiorite and gneiss. D2 lead to greenschist facies metamorphism of the rocks.

1. Introduction

The Bauolé-Mossi domain consists of predominately Palaeoproterozoic calc-alkaline and alkaline granitoid intrusions. These rocks were emplaced between ca 2.1 to 1.8 Ga (Vega et al., 2008). The presence of terranes that predates and may act as basement rocks to the Birimian granitoids has been the subject of debate. Basement rocks are typically gneissic to migmatitic, thus the granitoid-gneissic terranes in the West African Craton became the subject of a number of studies (Eisenhohr and Hirdes, 1992, Pons et al., 1995, Hirdes et al., 1996, Gasquet et al., 2003). Lemoine, 1988 in Gasquet et al., 2003 introduced the term Burkinian, which corresponds to reworking of Archean rocks and formed the gneissic terrance in Côte d'Ivoire. Hirdes et al., 1996 proposed the gneissic terrane in the Dabakala predate 2.1 Ga batholith intrusions. This was rejected by Gasquet et al., 2003 who concluded the gneiss were syntectonic despite zircons recovered at 2.3 Ga.

2. Regional Geology

The West African Craton consists of several shields. The Archean-Palaeoproterozoic Leo-Man rise in the south and the Reguibat rise in the north, which are separated by the Phanerozoic Toudeni basin. The Leo-Man rise consists of the Archean Kénéma-Man domain and the Palaeoproterozoic Baoulé-Mossi domain (Fig 2.1) (Cahen *et al.*, 1984).

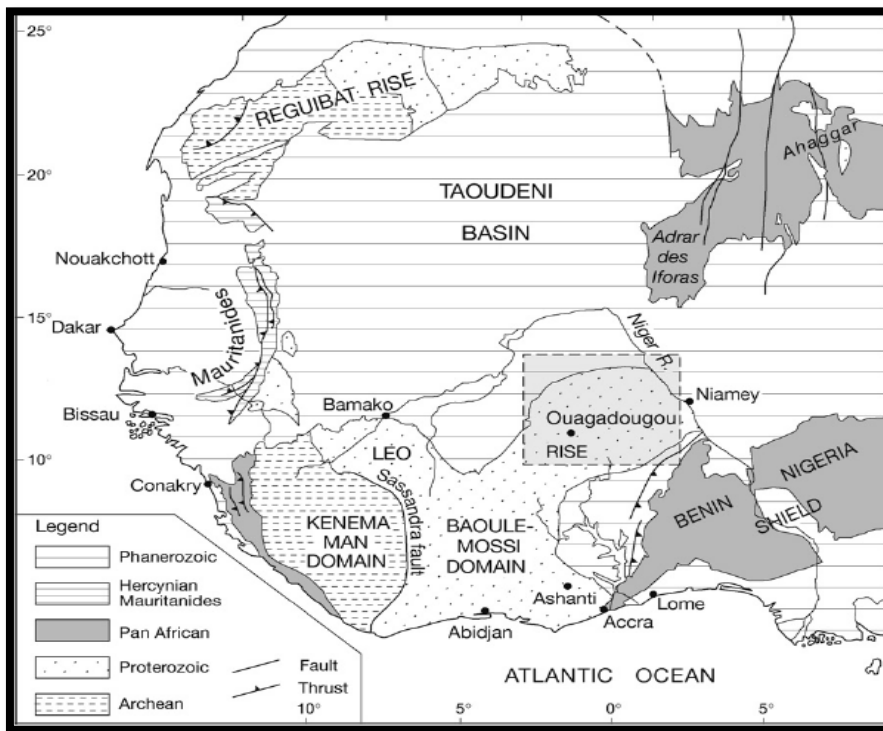


Fig 2.1. The West African Craton consists of the Archean and Palaeoproterozoic Reguibat in the north and the Leo-Man in the south (Béziat *et al.*, 2008).

2.1. Archean domain

The Archean domain is divided into three units -

- I. The basement rocks are grey-banded migmatitic orthogneiss, which formed ca. 3.5 to 3.4 Ga (Potrel *et al.*, 1998). The gneisses are trondhjemitic in composition (Kouamelan *et al.*, 1997). They were subsequently metamorphosed to granulite facies (Potrel *et al.*, 1998; Thieblemont *et al.*, 2004).
- II. The gneisses were then intruded by granitic batholiths ca. 2.7 Ga (Thieblemont *et al.*, 2004). The intrusions occur as granites (*sensu stricto*), crosscutting the basement gneiss (Kouamelan *et al.*, 1997).
- III. The basement rocks are overlain by metavolcanic and metasedimentary rocks of the Loko Formation (Feybesse and Milési, 1994).

The Kénéma-Man domain was deformed and metamorphosed during two major tectonic events. The Leonean cycle, ca 3.0 Ga is associated with north-south trending structures and metamorphism of basement rocks to granulite- facies (Cahen et *al.*, 1984; Thieblemont et *al.*, 2004). The Liberian event, ca 2.7 Ga resulted in N-S to NNE-SSW trending structures (Thieblemont et *al.*, 2004). The Liberian event culminated with TTG batholith intrusions (Skinner et *al.*, 2004).

2.2. Palaeoproterozoic Baoulé-Mossi domain

The Birimian was first described by Kitsh from outcrops in the Birim River Valley in southern Ghana (Pohl, 1998). The lithostratigraphic sequence became the subject of controversy, where two schools of thought emerged; the Anglophone and Francophone. Junner (from the Anglophone school) sub-divided the Birimian into the Lower and the Upper Birimian (Hirdes et *al.*, 1996).

- I. The Lower Birimian is predominately composed of metasedimentary rocks, including argillites, shale and conglomerates (Roddaz et *al.*, 2007). The metasedimentary rocks are intercalated with dacite and rhyolite metavolcanic rocks (Tshibubudze et *al.*, 2009).
- II. The Upper Birimian consists of tholeiitic lavas, which are locally pillowed, intercalated with turbidites and meta-volcanoclastic sedimentary rocks (Debat et *al.*, 2003).

The Tarkwaian unconformably overlies the Upper Birimian and consist of coarse clastic sedimentary unit (Tshibubudze et *al.*, 2009). The description of the unit is based on work done in Ghana (Eisenlohr and Hirdes, 1992).

- I. The Tarkwaian includes basal conglomerates from the Kewese Group (Pohl, 1998).
- II. Shales, quartzite and meta-conglomerates of the Banket Group.
- III. Overlying the Banket Group are shales and phyllites of the Tarkwa formation (Cahen et *al.*, 1984; Tshibubudze et *al.*, 2009).

The above Anglophone Birimian sequence was inverted by the Francophone school. The predominately volcanic units were interpreted as being younger than the metasedimentary units (Milési et *al.*, 1992). However, during a study of the Goren-greenstone belt in Burkina

Faso, Hein *et al.*, (2004) concluded that sub-dividing the Birimian into two units did not fit the conformable nature of the sequence. Instead, they found three intercalated meta-volcanic and meta-sedimentary sequences (Tshibubudze *et al.*, 2009). According to Tagini, (1971) in Hastings, (1982), the Birimian was deposited in an intra-continental rift basin, followed by sedimentation and localized volcanism. The Birimian and the Tarkwaian are considered to represent transition from a deep marine to sub-aerial depositional environment caused by uplift during craton accretion (Pohl, 1998).

2.3. Magmatic Intrusions

Granitoids cover approximately 70% of the Baoulé-Mossi domain (Debat *et al.*, 2003). The granitoids intruded into meta-volcanic and meta-sedimentary rocks during the Eburnean orogeny (Egal *et al.*, 2002). The Eburnean orogeny marks a major period of crustal thickening 2.1 to 2.0 Ga (Pons *et al.*, 1995).

The granitoids are calc-alkaline and locally alkaline in composition with minor crustal component (Gasquet *et al.*, 2003). The granitoids are divided into three groups, unfoliated hornblende-bearing, foliated biotite-bearing and alkaline granitoids (Dioh *et al.*, 2006). Gasquet *et al.*, (2003), Naba *et al.*, (2004) and Agbossoumonde *et al.*, (2007) observed that the granitoids grade into gneissic and migmatitic structures.

2.4. Regional tectonics

The Eburnean orogeny represents accretion of the Archean Kénéma-Man domain with the Palaeoproterozoic Baoulé-Mossi domain (Feybesse *et al.*, 2006). The orogeny is characterised by three deformation events, D1 and D2-D3 (Baratoux *et al.*, 2011). The deformation of the meta-volcano-sedimentary sequence was coeval to TTG granitoid and granite intrusions (Hein *et al.*, 2004).

According to Hirdes *et al.*, (1996) D1 deformation occurred between 2112 Ma to 2100 Ma. D1 magmatic event lead to metamorphism of the volcano-sedimentary sequence to greenschist and locally amphibolite facies (Baratoux *et al.*, 2011). D1 is also associated with the development of NW-trending folds (Hein *et al.*, 2004).

D2-3 represents a period of crustal thickening, which lead to NE-trending veins and brecciation (Tshibubudze *et al.*, 2009). Uplift and further shortening of the crust is associated with the development of brittle shears and NE-trending folds (Feybesse *et al.*, 2006).

Emplacement of the granitoids was parallel to NE-trending fold axial planes (Baratoux et *al.*, 2011).

3. Aim

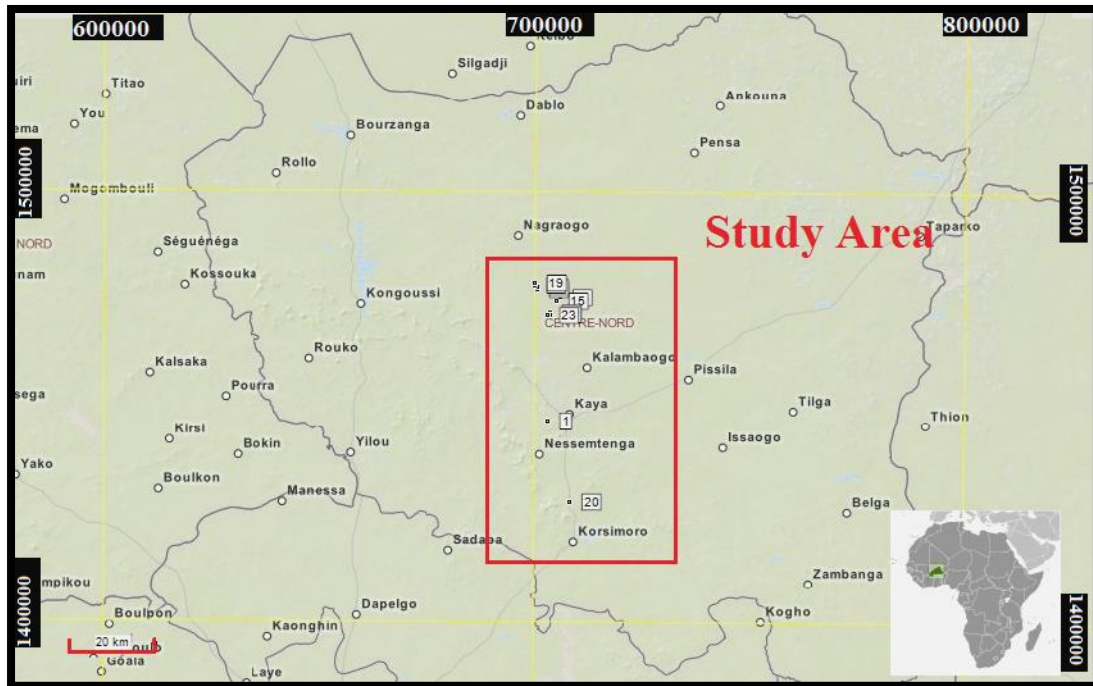


Fig 3.1. Map illustrates the location of the study area. The white numbers corresponds to sample numbers and the locations where each sample was collected.

The Pissila batholith and the Saaba zone gneiss are located near the town of Pissila in NE Burkina Faso. The aim of the project is to determine the relationship between the Pissila batholith and the Saaba zone gneiss. The gneiss could represent a highly metamorphosed and deformed part of the batholith. On the other hand, the gneiss may be a partially exposed gneissic terrane that has little to no affiliations to the batholith. The contact between the two could not be established during fieldwork due to lack of outcrops.

The relationship between the Pissila batholith and the Saaba zone gneiss is determined by;

- I. Providing a petrographic and geochemical description of the batholith and the gneiss.
- II. Comparison of the petrographic and geochemical data obtained for the two areas.
- III. Comparison batholith and the gneiss with other granitoids in Burkina Faso and similar granitoids in the West African Craton.

4. *Methodology*

Field work

Samples from the Pissila batholith and the Saaba Zone gneiss were collected during field work in January 2012. Mapping of the study area and sample collection was conducted by Profs. Kerstin Saalman and Kim Ncube-Hein. The locations of each station point were recorded using GPS co-ordinates. The World Geodetic System (WGS 84) and Universal Transverse Mercator (UTM) in meters were used as the datum and format, respectively. The location map of the study area was created using Expert GPS 4.57. The data from Expert GPS was exported to Google Earth.

Petrography

Seven polished thin sections were used for petrography. Reflected light was used to examine the oxide mineralization. Five of the seven thin sections were used for point counting. An average of 500 minerals in each samples were counted using Petrog JVC V2.42.15. The data obtained from point counting was used for sample classification and comparison.

Thin sections were photographed under transmitted light. The coarse nature of some of the samples did not allow for the foliation to be photographed. Thin sections were subsequently scanned to illustrate the foliation.

Geochemistry

Five samples were submitted for geochemical analysis. The bulk composition of the rocks was obtained using Wavelength Dispersive X-ray Fluorescence Spectrometry (WDXRF) and Inductively coupled plasma emission mass spectrometry (ICP-MS). Samples were crushed and finely milled for both methods.

Major elements were analyzed using WDXRF from fused disks. The milled samples were mixed with a pre-ignition flux and heated to 1,020°C for 50 minutes. H_2O^- and H_2O^+ were then calculated. The mixture was mechanically pressed into a fused disk and analyzed.

Samples for ICP-MS were prepared by mixing the milled powder with HNO_3/HF and heated to 235°C. The liquid was evaporated on a hot plate that was heated to 70°C. 2ml of

HNO₃ was added to the liquid and heated to 60°C and evaporated. The evaporated sample was then ready for ICP-MS.

5. Petrography

5.1. Granodiorite

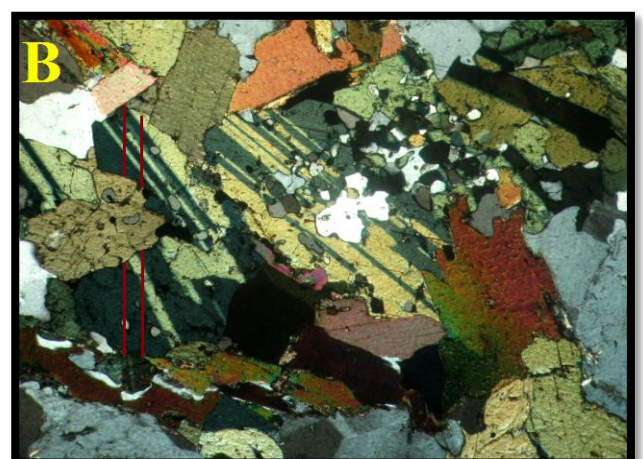
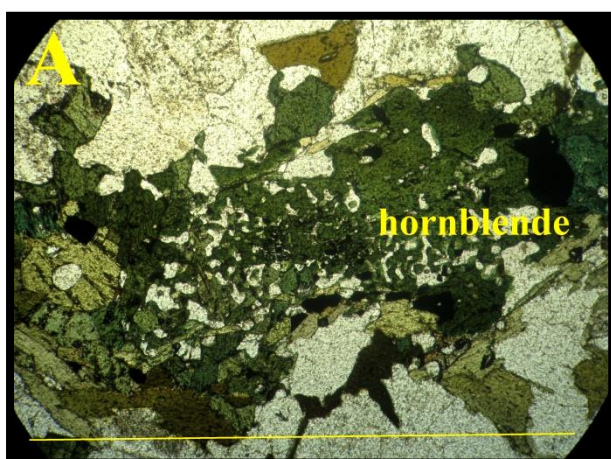
Granitoid sample, KS-2012-14 and KS-2012-15 are coarse-grained granodioritic rocks. Both samples were used for hand-sample description, but only KS-2012-15 was used for thin-section description. In hand specimen, the rocks have a dark greenish colour. The colour is due to the abundant hornblende and biotite. Sample KS-2012-15 contains hornblende (16%), biotite (9%), plagioclase (24%), quartz (35%) and microcline (15%). Accessory minerals are Fe-Ti oxide, chlorite and epidote (>1%) (Table 1). The granitoid, based on modal abundance, is classified as granodiorite (Appendix E).

Hornblende in sample KS-2012-15 is anhedral and zoned. The minerals exhibit a graphic texture between hornblende, quartz and Fe-Ti oxide (Fig 5.1.1 A). Hornblende has twinning lamellae that is oblique to cleavage (Fig 5.1.1B).

Primary and secondary biotite was found in the sample. Secondary biotite occurs in replacement of hornblende. The minerals are fine-grained and exhibits serrated grain-boundaries. Primary biotite exhibit lobate grain-boundaries. It also exhibit folded cleavage, undulose extinction and fractures (Fig 5.1.1C).

Plagioclase, microcline and quartz are weakly foliated. Plagioclase crystals are subhedral, anhedral and very coarse. Microcline is associated with lobate myrmekite. Myrmekite was found on the shortening axis of microcline. Quartz exhibits strain induced deformation bands (Fig 5.1.1 D).

The foliation in the granodiorite is defined by a weak alignment of hornblende, biotite and quartz-feldspathic minerals. Quartz and microcline exhibit an alignment that is sub-parallel to the mafic minerals. Myrmekite between quartz and microcline was found on the shortening axis of microcline. Plagioclase exhibits preferred orientation in two directions, parallel and oblique to the mafic minerals.



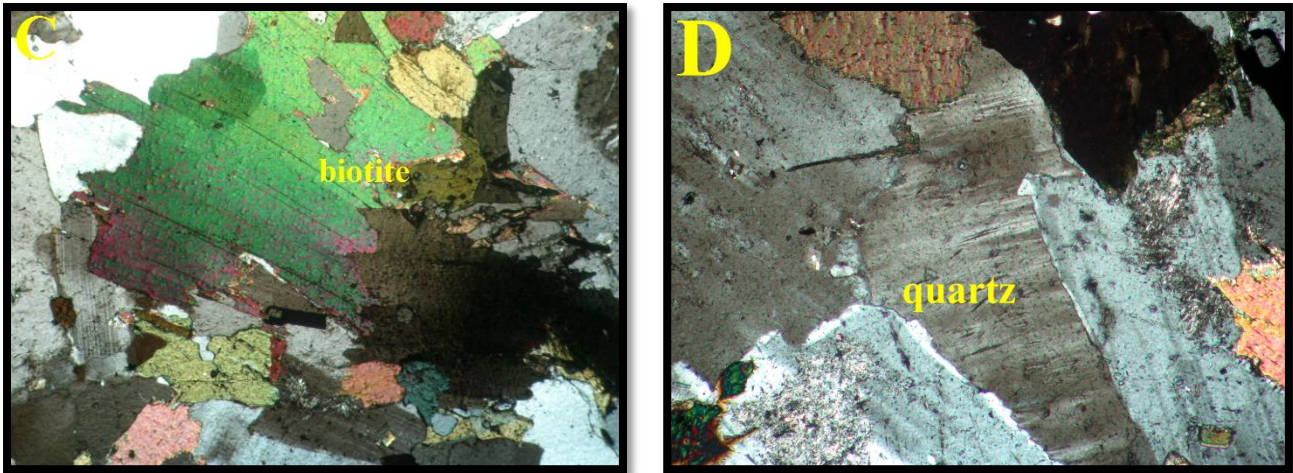


Figure 5.1.1. (A) Primary intergrowth between hornblende, quartz, plagioclase and Fe-Ti oxide. (B) Hornblende with twinning lamellae that is oblique to cleavage. Cleavage direction is indicated with yellow lines. (C) Illustrates biotite with folded cleavage and undulose extinction. (D) Quartz in the centre exhibit deformation bands.

5.2. Biotite gneiss

The Saaba Zone is characterised by medium-grain biotite gneiss. Hand samples KS-2012-17B and 17C are foliated. Biotite, hornblende and discontinuous feldspathic layers (0.5-3mm thick) define the fabric. Sample KS-2012-17B is predominately composed of quartz (66%) with plagioclase (18%), microcline (8%), hornblende (3%), biotite (5%) and Fe-Ti oxide (>1%) (Table 1).

Hornblende and biotite are elongated and strongly aligned. The minerals form parallel and anastomosing foliations. The minerals are associated with Fe-Ti oxide. Oxides are cubic, which indicates primary mineralization. Oxides are also found over-printing biotite.

Quartz, plagioclase and microcline are elongated. The minerals are aligned sub-parallel to biotite. Low temperature structures that include pressure solution and sweeping undulose extinction are prevalent in quartz. However, minor amount of chessboard quartz was found in the samples (Fig 5.2.1A). Plagioclase and microcline are dominated by grain-size reduction and sub-grain rotation (Fig 5.2.1B).

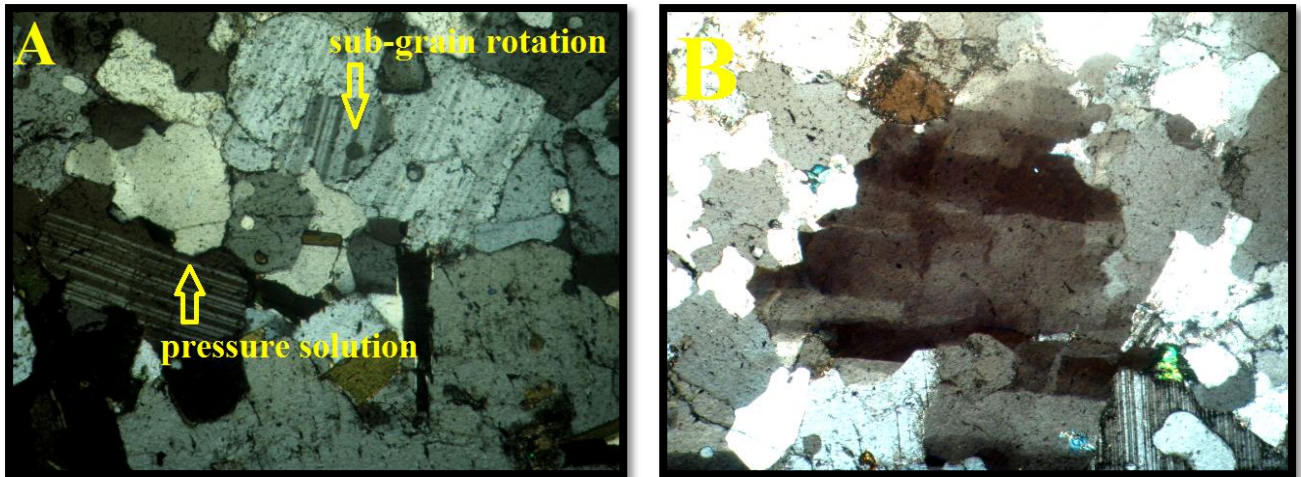


Figure 5.2.1 (A) The image illustrates the formation of sub-grains and subsequent rotation of the sub-grains. The image also shows pressure solution. (B) Chessboard sub-grains in the samples occur in minor amounts.

5.3. Migmatites

Migmatites are a mixture of two or more petrographically distinct parts (Sawyer, 2008). They form by partial melting of a source rock. The melt forms light-coloured veins (leucosome) and mafic-rich melanosomes. The Saaba Zone gneiss is locally migmatitic. Foliation and small-scale folds are visible in hand samples. In hand sample, the leucosomes are composed of discontinuous quartz and feldspar-rich melts. The melanosomes are predominantly composed of biotite and hornblende.

The folds in Sample KS-2012-23 consist of predominantly biotite with minor hornblende and Fe-Ti oxide. Biotite is cross-cut by acicular rutile. Rutile suggests late Ti-rich hydrothermal fluid circulation. Fe-Ti oxide is also associated with biotite.

Plagioclase and microcline were found with pervasive sericitic alteration (Fig 5.3.1 A, B). Microcline and plagioclase twinning lamellae were not visible due to pervasive alteration. In plane polarized light quartz exhibit “cloudy” texture as a result of numerous fluid inclusions.

The migmatites are cross-cut by K-feldspar rich veins. In hand sample, the veins exhibit a grainy-texture. The vein is predominantly composed of quartz, minor microcline and less than 1% plagioclase. Biotite was found interstitial to quartz and microcline or found as clusters.

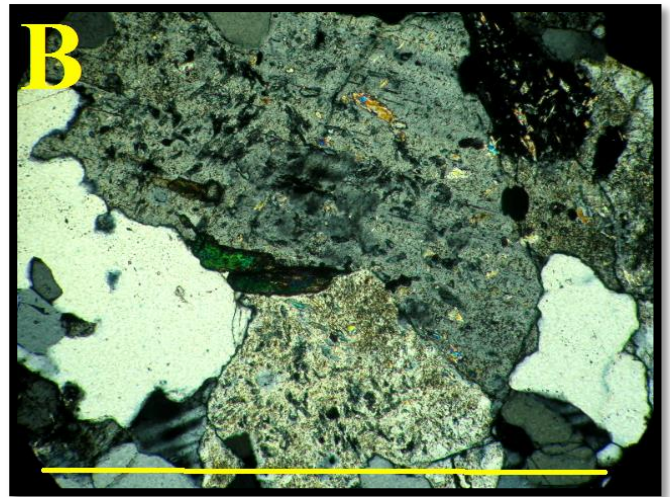
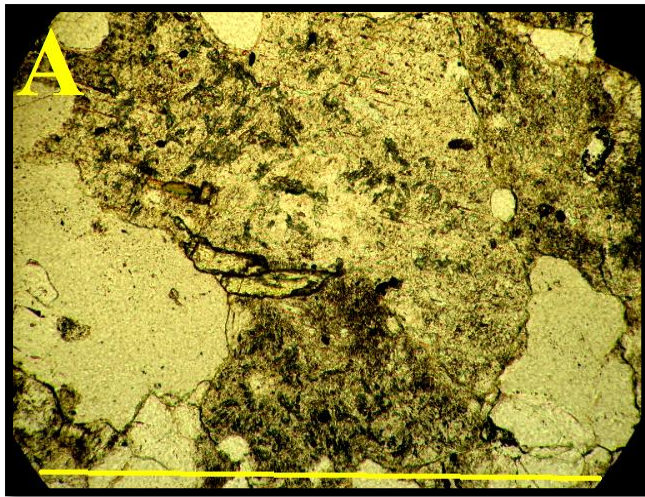


Figure 5.3.1 (A) Image shows altered K-feldspar in plane polarized light. (B) The same image as (A) now in crossed polarized light.

Table 1.

Modal abundance (normative).

Minerals	KS-2012-15 (granodiorite)	KS-2012-17B (bt-gneiss)	KS-2012-22 (migmatite)	KS-2012-23 (migmatite)	KS-2012-21 (migmatite)
Plg	24	18	10	4	3
Kfs	15	8	37	16	50
Qtz	35	66	40	67	37
Hbl	16	3	5	4	1
Bt	9	5	7	7	7
Oxide	1	<1	1	1	2
Chl				<1	<1
Mus				<1	<1
Total	100	100	100	99	100

plg=plagioclase; kfs= microcline; qtz=quartz; hbl=hornblende; bt=biotite;
chl=chlorite; mus= muscovite.



Fig. 5.4.1. Foliated coarse-grained granodiorite. The rock consists of hornblende, biotite, plagioclase, microcline, quartz, epidote, chlorite and Fe-Ti oxide.



Fig 5.4.2. Gneiss exhibits folded leucocratic veins in hand sample. The leucocratic veins consists of coarse-grained quartz, plagioclase and microcline.



Fig 5.4.3. The image illustrates migmatite with leucosome. The leucosome consists of biotite and hornblende cluster that give the vein a spotted texture.

6. *Geochemistry*

Geochemistry is one of the fundamental steps in understanding magmatic rocks. It allows for understanding of the source material, processes that form and influence the evolution of the rocks. The chemical signature of metamorphic rocks is predominately influenced by the composition of the parent rock. It is possible that the composition of the metamorphic rock is derived from a mixture of two sources.

In this section the aim is to compare and contrast the geochemical data of the granodiorite, K-rich vein and gneiss/migmatites. The geochemical data is divided into two groups, major and trace elements. A comparison on the samples collect with those in the Birimian follows in the discussion.

6.1 *Major elements*

The granodiorite exhibit a slightly acidic composition ($\text{SiO}_2 = 64.83$ wt %). The gneiss and migmatites exhibit higher silicate oxide content, which ranges from 74.01 to 75.61wt %. The granodiorite was classified as a quartz-monzodiorite/ monzogabbro. Gneiss and migmatites were classified as granodiorite and trondhjemite, respectively. This classification is based on CIPW norm mineral calculations (Fig 6.1.1). On the other hand, the samples have a different classification when using the sample's alkali and silicate content (Fig 6.1.2).

Granodiorite is more mafic rich compared to the other samples. The iron content in granodiorite is almost twice that of gneiss and the K-rich vein. In general the granodiorite has the highest oxide content (Table 2).

The K-rich vein, in contrast to the granodiorite exhibit low oxide percentage in all major elements. However, the SiO_2 and K_2O content are highest in the vein. Gneiss and migmatites generally exhibit composition that plots in between the granodiorite and K-rich vein.

The samples are medium to high K calc-alkaline, except one migmatite sample that has a low K tholeiitic composition. $\text{Na}_2\text{O}/\text{K}_2\text{O}$ ratio in gneiss and migmatites range from 2.09 to 4.52. Granodiorite and K-rich $\text{Na}_2\text{O}/\text{K}_2\text{O}$ ratios are 1.32 and 0.87, respectively. $\text{K}_2\text{O}/\text{Na}_2\text{O}$ ratios in all samples are less than 0.5, with exception to granodiorite and K-rich vein.

Table 2.

Analytical data obtained from XRF.

Samples	KS-2012-15 (granodiorite)	KS-2012-17B (bt-gneiss)	KS-2012-17C (bt-gneiss)	KS-2012-18B (K-rich vein)	KS-2012-23 (migmatite)
SiO ₂ (wt %)	64.83	74.77	75.62	78.37	74.01
Al ₂ O ₃	15.49	12.93	12.81	11.89	13.6
Fe ₂ O ₃	0.53	0.27	0.23	0.11	0.32
FeO	4.33	2.22	1.9	0.86	2.58
MnO	0.08	0.05	0.05	0.01	0.07
MgO	2.76	0.46	0.37	0.09	0.54
CaO	4.46	1.89	1.74	0.89	2.46
Na ₂ O	3.94	4.85	4.63	3.55	5.02
K ₂ O	2.98	1.77	2.22	4.05	1.11
TiO ₂	0.5193	0.2824	0.2314	0.0551	0.3276
P ₂ O ₅	0.22	0.07	0.06	0.03	0.1
Cr ₂ O ₃	0.018	0.0036	0.0059	0.0008	0.0034
NiO	0.005	0.0026	0.0005	0.0002	0.0007
Total	100.16	99.57	99.87	99.91	100.15
LOI	0.76	0.47	0.46	0.68	1.19
Sc (ppm)	9.18	7.4	6.79	0.59	9.08
V	87.03	16.25	11.18	1.64	19.75
Cr	57.73	4.68	2.07	1.05	8.96
Co	15.54	0.97	3.28	2.43	6.58
Ni	21.02	3.32	0.57	1.24	4.32
Cu	13.23	1.62	3.48	3.68	6.12
Zn	50.17	40.47	30.58	10.03	43.44
Ga	17.47	16.72	14.59	12.7	17.35
Rb	68.9	44.06	45.79	63.37	28.75
Sr	711.84	91.47	92.46	87.25	129.93
Y	12.58	32.47	26.96	12.19	40.87
Zr	134.05	155.56	142.8	82.08	149.75
Nb	4.28	9.14	7.37	0.6	8.61
Mo	0.6	0.78	1.12	0.37	0.18
Ba	927.62	275.92	397.71	572.58	262.05
Pb	7.44	5.98	4.99	6.43	2.36
Th	5.28	2.36	1.03	6.08	0.25
U	0.42	1.41	2.03	0.79	1.1

Table 3.

CIPW norm using major elements.

Normative mineral	KS-2012-15 (granodiorite)	KS-2012-17B (bt-gneiss)	KS-2012-17C (bt-gneiss)	KS-2012-18B (K-rich vein)	KS-2012-23 (migmatite)
qtz	15.45	33.75	34.8	39.55	32.93
plg	49.24	49.32	46.79	34.39	53.77
orth	17.37	10.46	13.12	23.93	6.56
diop	4.29	0.62	0.62		0.31
hyp	11.54	4.31	3.61	1.63	5.24
ilm	0.99	0.53	0.44	0.11	0.63
mgt	0.77	0.39	0.33	0.16	0.46
apt	0.51	0.16	0.14	0.07	0.23
Zir	0.03	0.03	0.03	0.01	0.03
cor				0.07	
chr	0.01				
Total	100.2	99.57	99.88	99.92	100.16

qtz=quartz; plg= plagioclase; diop=diopside; hyp=hpyersthenes; ilm=ilmenite;
mgt=magnetite; apt=apatite; zir=zircon; chr=chromite; cor=corundum

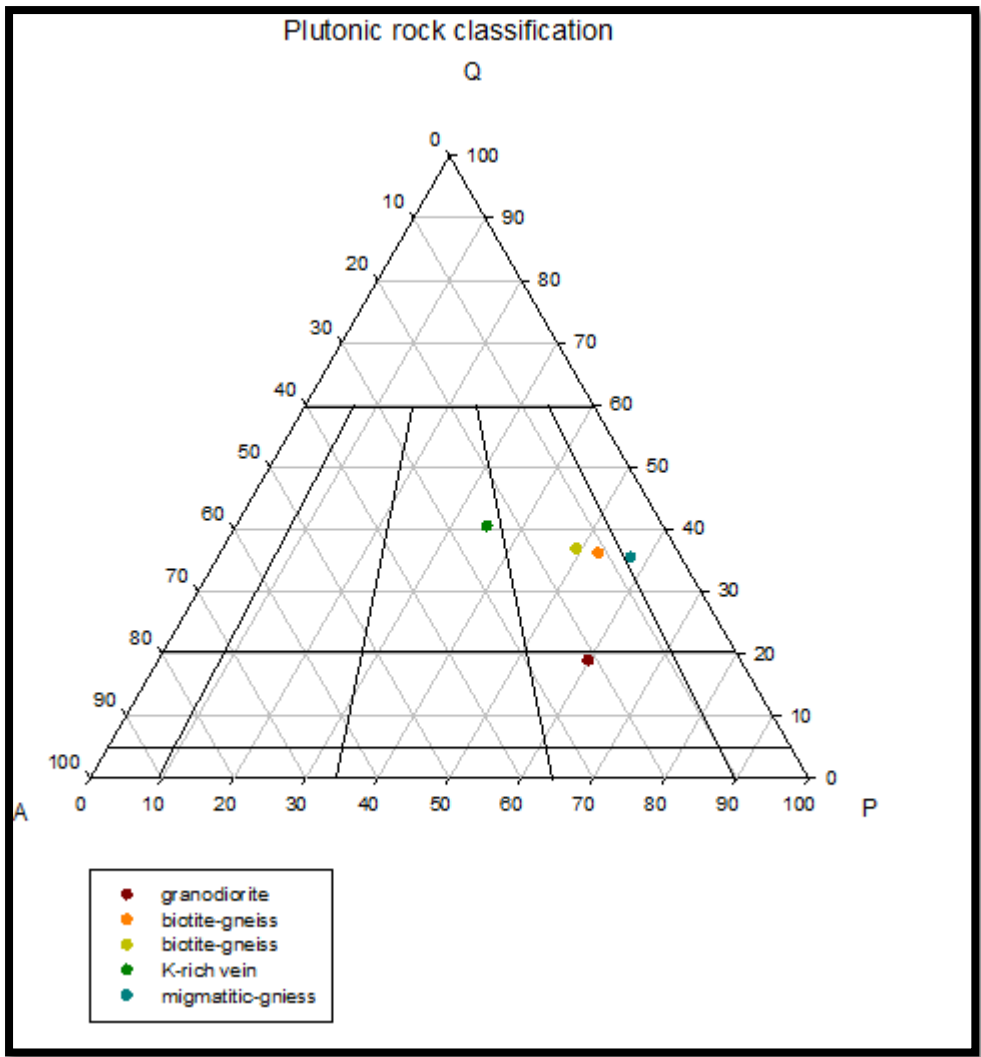


Fig. 6.1.1. Plutonic rock classification diagram based on CIPW norm minerals

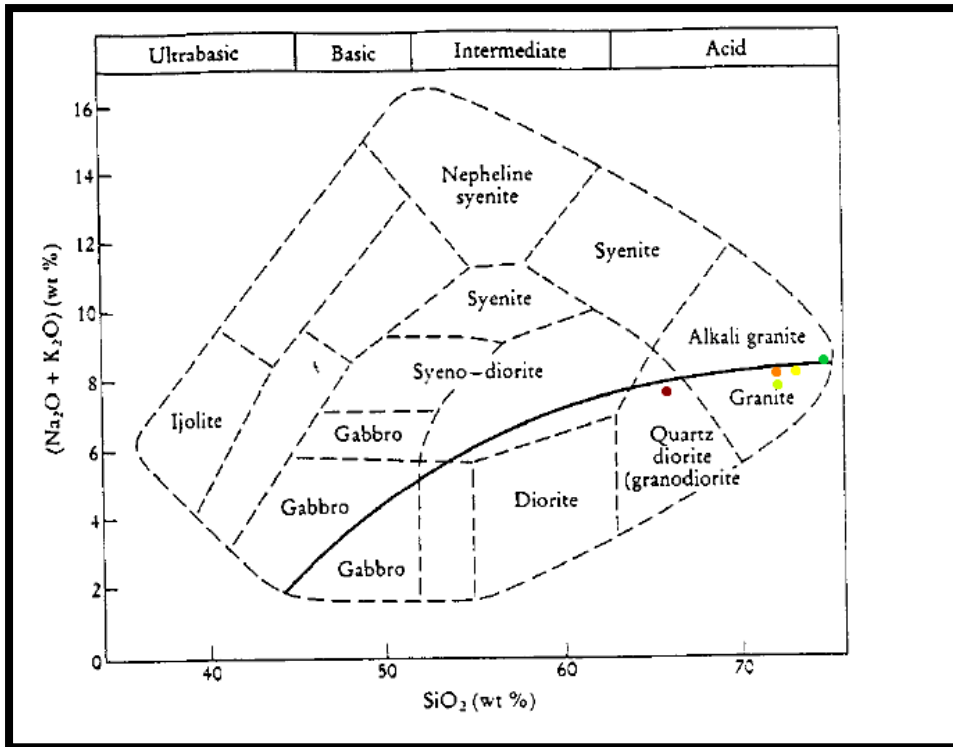


Fig 6.1.2. The alkali verse silicate oxide diagram illustrates that sample KS-2012-15 is granodioritic in composition. The gneiss and migmatites have a granitic composition and the K-rich vein is an alkali granite. (Maroon= granodiorite, yellow and orange= biotite- gneiss, green=K-rich vein, blue= migmatite).

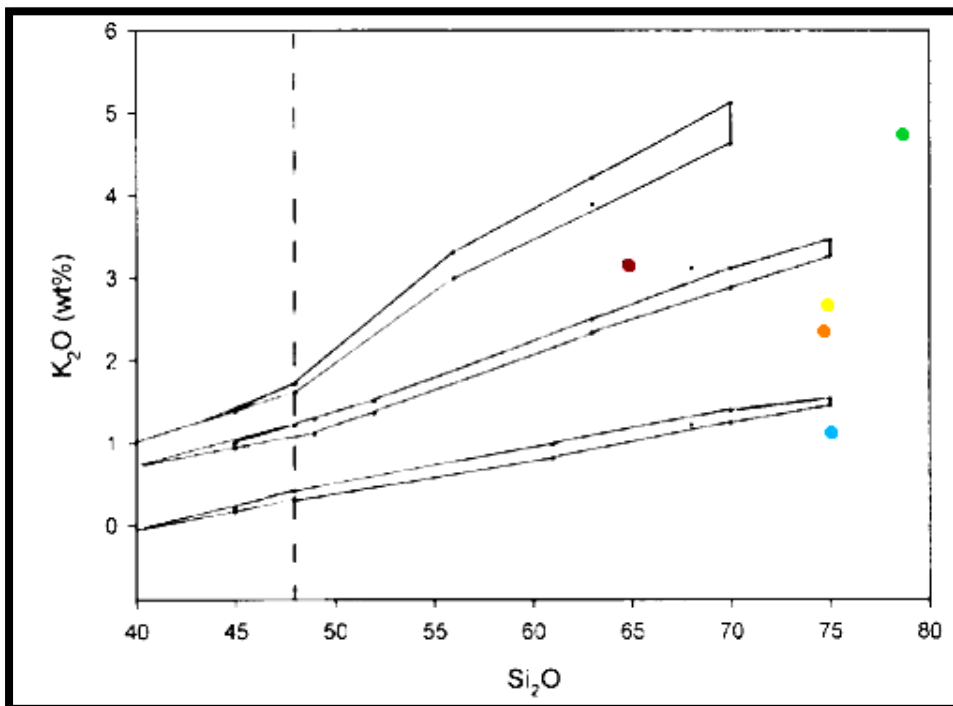


Fig. 6.1.3. The diagram illustrates that samples are medium- to high K calc-alkaline series, except one migmatite sample that is low K tholeiite. (Maroon= granodiorite, yellow and orange= biotite- gneiss, green=K-rich vein, blue= migmatite).

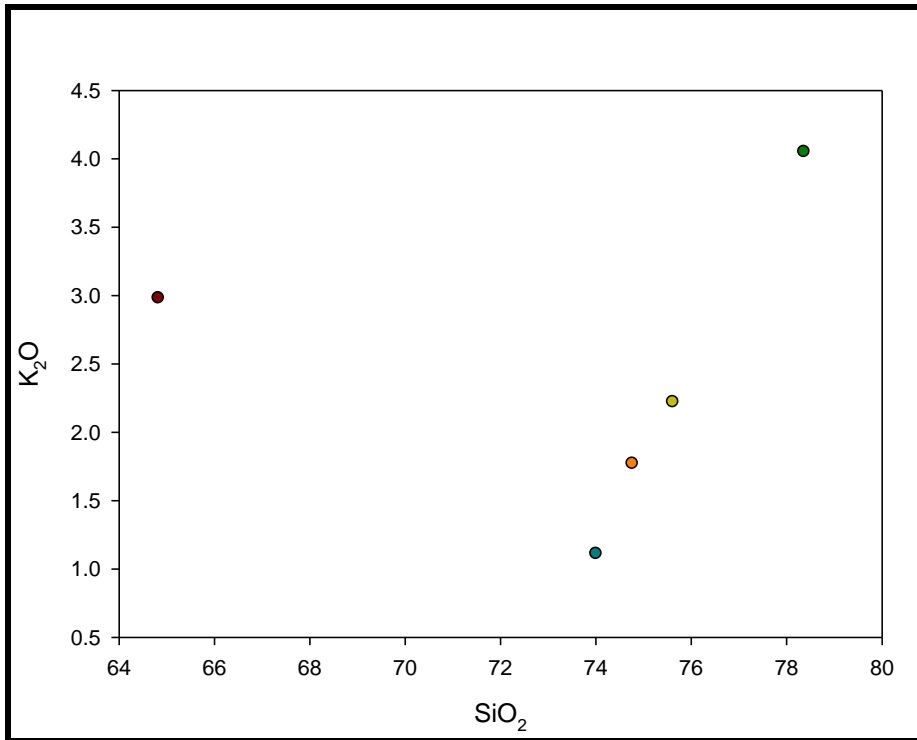


Fig.6.1.4. K-rich vein exhibit high K₂O and high Si₂O content. Gneiss and migmatites K₂O ranges from 1.11 to 4.85wt %. (Maroon= granodiorite, yellow and orange= biotite- gneiss, green=K-rich vein, blue= migmatite).

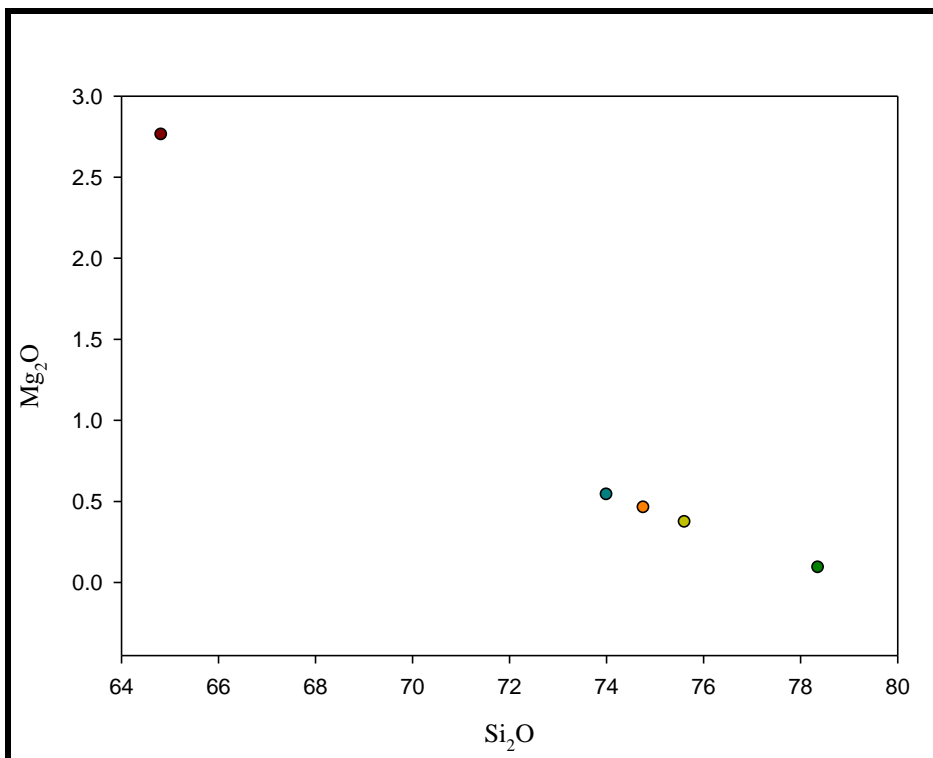


Fig. 6.1.5. Gneiss and migmatites exhibit composition that lies between granodiorite and K-rich vein. (Maroon= granodiorite, yellow and orange= biotite- gneiss, green=K-rich vein, blue= migmatite).

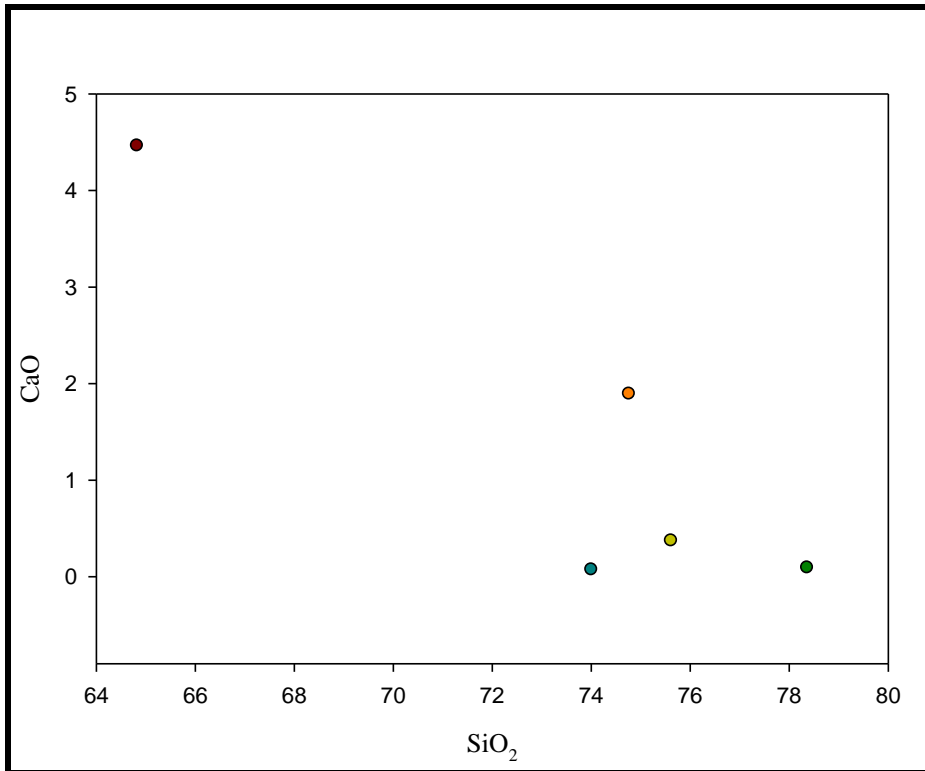


Fig. 6.1.6. Granodiorite exhibit relatively high CaO content relative to the other samples that exhibit low CaO. (Maroon= granodiorite, yellow and orange= biotite- gneiss, green=K-rich vein, blue= migmatite).

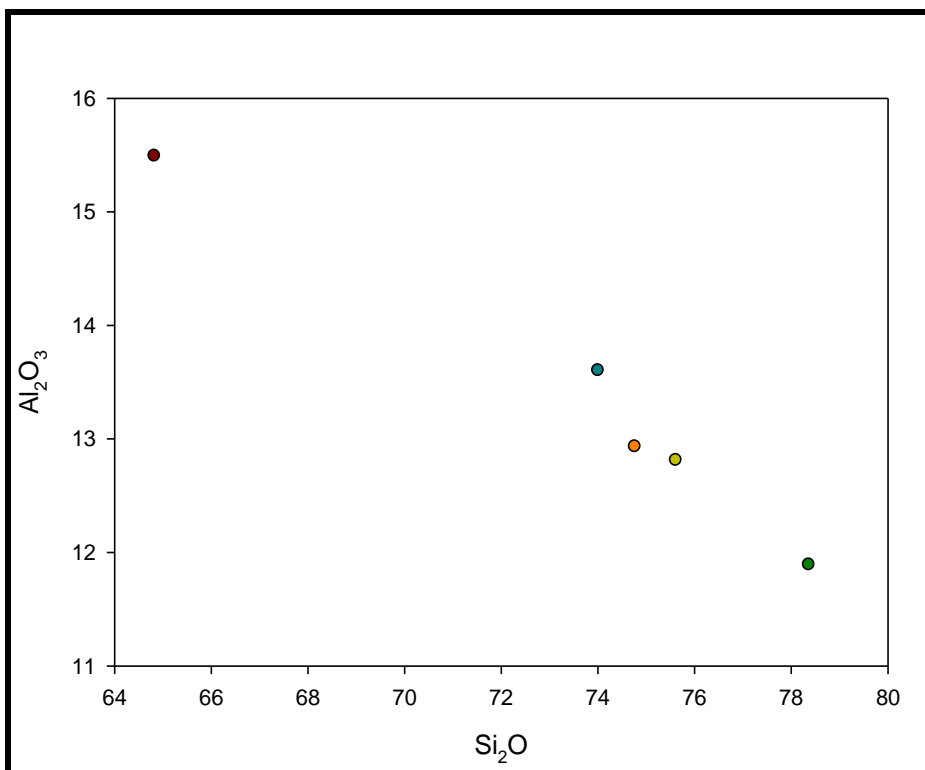


Fig. 6.1.7. Gneiss and migmatites exhibit composition that lies between granodiorite and K-rich vein. (Maroon= granodiorite, yellow and orange= biotite- gneiss, green=K-rich vein, blue= migmatite).

6.2. Trace Elements

The granodiorite exhibit a depleted rare earth element pattern (REE) relative to the gneisses and K-rich vein. The granodiorite is depleted in heavy rare earth elements (HREE) and enriched in light rare earth elements (LREE) (Fig 6.2.1.). The samples exhibit no Eu anomaly and exhibit a negative Ce anomaly. The granodiorite also exhibit a slight negative Tm anomaly. Large ion lithophile elements (LILE) are enriched relative to high field strength elements (HFSE) (Fig 6.2.3.). Granodiorite spider plot differs from gneisses, migmatite and K-rich vein (Fig 6.2.2). The granodiorite does not exhibit negative Sr and P anomaly, which are found in the other samples.

The gneisses, similar to the granodiorite are enriched in LREE and depleted in HREE (Fig 6.2.1). The gneisses REE pattern is enriched relative to the granodiorite, migmatite and K-rich vein. The samples exhibit a negative Eu anomaly. The samples have concave up ends, which are similar to granitoid in the region. The samples are enriched in LILE relative to HFSE (Fig 6.2.3). The spider plot exhibit similarities with the samples from the Dabakala region in Côte d'Ivoire that were described by Gasquet *et al.*, 2003 (Fig 6.2.2 and appendix 1). The gneisses in the spider plot exhibit a prominent negative Ti and P anomaly.

The migmatite exhibit a REE pattern that is relatively flat (Fig 6.2.1). The sample's REE pattern is depleted relative to the granodiorite, gneisses and K-rich vein. The flat REE pattern suggests that the migmatite's source rock lacked garnet. The presence of garnet in the source would have produced a depleted HREE pattern relative to LREE. Similar to gneisses the sample exhibits a negative Eu anomaly. The migmatite exhibits a positive Ce anomaly and a negative Eu anomaly. Similar to the above samples, the migmatite is enriched in LILE relative to HFSE.

The K-rich vein is depleted in LREE relative to HREE (Fig 6.2.1). The sample exhibits a negative Eu anomaly and a slight negative Ce anomaly. The HREE end is concave up. The sample exhibits an enrichment in LILE relative to HFSE (Fig 6.2.3). The K-rich vein's spider plot matches that of gneiss, except the K-rich vein's negative anomalies are more pronounced.

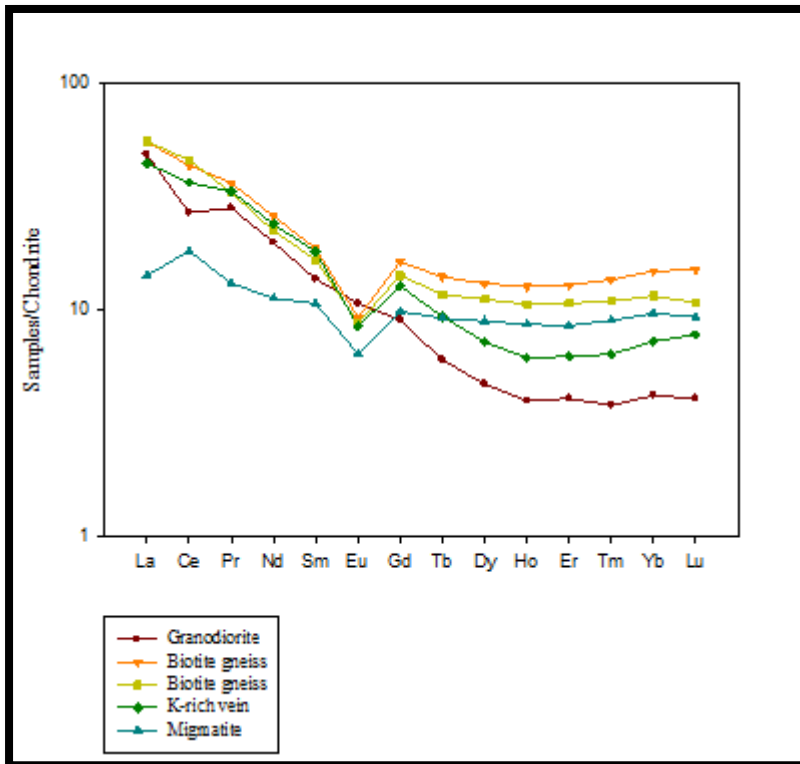


Fig. 6.2.1. REE plot of the gneiss and K-rich vein are comparable. The granodiorite and migmatites exhibit REE pattern that differ from the gneiss. This may indicate the samples are not related to each other. Normalising values from Evensen et al., 1978

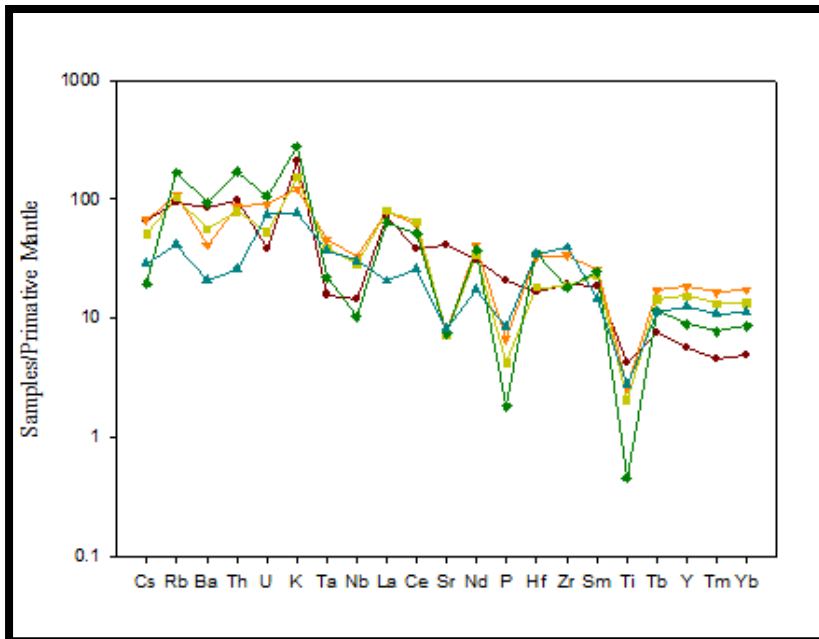


Fig 6.2.2. The spider diagram illustrates similar patterns between gneisses, migmatites and K-rich vein. The gneiss and granodiorite exhibit different anomalies, which may indicate that the samples were not derived from the same source. Normalising values from Thompson (1982) and from Sun (1980) for Rb, K, P, U, Cs.

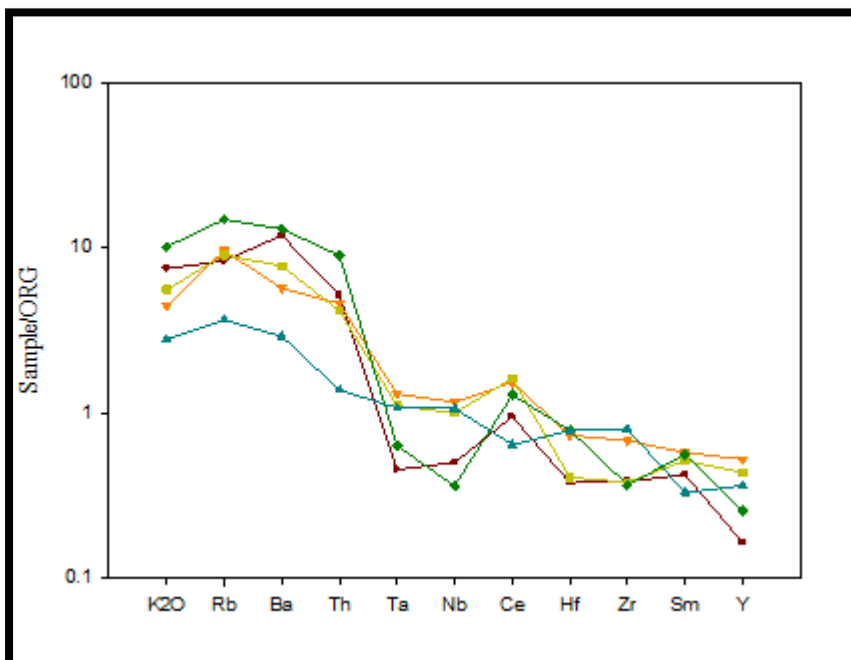


Fig. 6.2.3. Samples exhibit an enrichment in LILE relative to HFSE. This is generally associated with metasomatisation of the source rock (Rollinson, 1993). Normalising values from Pearce et al., (1984) in Rollinson, 1993.

7. Discussion

7.1. Comparison between the gneiss and granodiorite

The Pissila batholith and the Saaba zone gneiss are petrologically and geochemically different from each other. The granodiorite exhibit a composition that is more mafic relative to the gneiss and migmatite. This is apparent in the thin section where hornblende and biotite are dominant in the granodiorite relative to the gneiss and migmatite. In general, the granodiorite exhibit higher oxide content relative to the gneiss and migmatite, with an exception to SiO₂ and K₂O.

The K-rich vein exhibit a similar REE slope and pattern to the gneiss. This may indicate that the K-rich vein was derived from a source comparable to the gneiss. Granodiorite exhibit a steep REE slope, whereas gneiss, migmatite and K-rich vein exhibit a flat slope. The gneiss and K-rich vein are enriched in REE relative to the granodiorite. On the other hand, migmatite is depleted in REE relative to the other samples.

The spider diagram exhibit variations between the gneiss and granodiorite. Granodiorite exhibit a positive Sr anomaly, while other samples exhibit a prominent negative Sr anomaly. The gneiss, migmatite and K-rich vein also exhibit negative Ti, P and Ba anomalies. The granodiorite exhibits either a weak negative or no Ti, P, Ba anomalies.

The samples exhibit some geochemical similarities. All samples exhibit an enrichment of LILE relative to HFSE. This may indicate metasomization of the source rock (Rollinson, 1993). The samples are depleted in HREE relative to LREE, which indicates a garnet and amphibolite-bearing source rock or residuum (Holland & Turekian, 2003). Migmatites exhibits a flat REE slope, which may suggests that garnet and amphiboles had a minor role melt production.

7.2. Gneiss and migmatite

The migmatites exhibit some similarities to Archean TTG. The samples exhibit SiO₂> 70 wt%, Na₂O/K₂O>0.5, K₂O/Na₂O<0.5, which is characteristic of Archean TTG (Clarke, 1992). Thus the gneiss and migmatite may have formed from processes similar to those that form Archean TTG. In contrast to the TTG described by Smithes, (2000), the Saaba zone gneiss and migmatites do not exhibit low Al₂O₃, Sr and Ba less than 500ppm.

Archean TTG are thought to have formed by partial melting of a hydrated oceanic crust or partial melting of a thickened crust, leaving a garnet-bearing amphibolite residuum (Martin and Moyen, 2002). The latter is not favoured to produce Archean TTG (Martin *et al.*, 2005). The TTG are thought to represent felsic melt that interacted with the mantle during diapiric ascent (Clarke, 1992). Partial melting of the lower thickened crust could not have allowed the melt to interact with the mantle prior to emplacement (Smithes, 2000).

According to Doumbia *et al.*, 1998, the concave up HREE end is typical of Archean TTG and of calc-alkaline granitoids in the region. Depletion of HREE relative to LREE is controlled by garnet and amphiboles retained in the residuum (Rollinson, 1993). The negative Eu and Sr anomalies suggest that plagioclase was retained in the residuum or plagioclase was removed from the melt during magma differentiation (Holland & Turekian, 2003).

The spider diagram is enriched in LILE relative to HFSE, which suggests metasomatisation of the source rock (White, 2012). The negative Ti, Ta, Nb anomalies are associated with Ti-bearing mineral phases in the residuum (Rollinson, 1993). The Ta-Nb anomalies in gneiss, migmatites and the K-rich vein are considered to be an indicator of crustal contamination (Holland & Turekian, 2003).

7.3. *Granodiorite*

The granodiorite was probably derived from partial melting of a metasomitized garnet-bearing amphibole with a crustal component. Emplacement of the granitoid was between 2143 ± 12 and 21117 ± 17 Ma in an island arc setting. The granitoid was later deformed and metamorphosed to greenschist facies during the Eburnean orogeny (Tshibubuze *et al.*, 2009).

The composition of igneous melts is controlled by the chemical composition of the source, differentiation during magma ascent and trace element compatibility with the mineral phase. The depletion of HREE relative to the LREE is controlled by HREE partitioning into garnet, hornblende and pyroxenes (White, 2012). According to Doumbia *et al.*, 1998, this indicates that the granodiorite melt was derived from partial melting of oceanic lithosphere at pressures where garnet and amphiboles are stable. The negative Nb-Ta anomaly is widely regarded as an indicator of subduction and crustal contamination (Fig 6.2.3.) (Rollinson, 1993). Metasomization of oceanic lithosphere is considered to be the cause the LILE enrichment relative to HFSE in the granodiorite (Holland & Turekian, 2003).

The spider diagram of the studied granodiorite is comparable with spider diagrams for the Dabakala region in Côte d'Ivoire (appendix 1) (Gasquet *et al.*, 2003). The diagrams exhibit negative Ta, Ti and Nb, which are usually associated with titaniferous minerals retained in the residuum (White, 2012). A negative Ce and Nb anomaly is generally regarded as an indicator of crustal contamination (fig 6.2.2.) (Rollinson, 1993). The positive Sr anomaly attests to declining role of plagioclase in melt production (Holland & Turekian, 2003). The positive Sr coupled with Eu anomaly, indicates that plagioclase was not retained in the residuum during partial melting or fractionated during magma differentiation (Rollinson, 1993; Holland & Turekian, 2003).

7.4. *Deformation and metamorphism*

Metamorphism and deformation leads to mineralogical and structural changes in the rock. The two occur in response to temperature, pressure and fluid variations. The processes lead to changes in mineral phase, shape, orientation and grain-size.

Gneiss and migmatite

The mineral assemblage in the gneisses and migmatites (hornblende, biotite, quartz, plagioclase, microcline, epidote, chlorite and muscovite) suggests metamorphism to amphibolite and greenschist facies. The low microstructures in the gneiss and migmatites are similar to those in granodiorite. However, high temperature microstructures were observed in the gneiss and migmatites. The occurrence of both high and low temperature metamorphic minerals and microstructures indicates at least two deformation events (D1-D2). The first deformation event (D1) lead to amphibolites facies metamorphism and was followed by D2. D2 lead to the development of low temperature overprint.

The samples exhibit cataclasis of feldspar, plagioclase and quartz. This occurs at temperature below 300°C. (Pryer, 1993). Other low temperature microstructures (including bulging, sub-grain rotation and sub-grain formation) observed in the gneiss and migmatites are similar to microstructures in granodiorite. Theses microstructures are discussed in detail in the following section.

The gneiss and migmatites were found to preserve microstructures that indicate high metamorphic temperatures. The samples exhibit an increase in sub-grain formation and rotation relative to the granodiorite. According to Stipp *et al.*, 2002 an increase in sub-grain formation and rotation is attributed to an increase in temperature, where grain boundary

migration becomes the dominate feature. The development of quartz with chessboard extinction occurs during inversion of α -quartz to β -quartz which occurs at $630^{\circ} \pm 30^{\circ}\text{C}$ (Kruhl, 1996). Based on quartz with chessboard extinction metamorphic temperatures that the gneiss and migmatites experienced where at least 630°C .

Granodiorite

Subsequent to magma emplacement and crystallisation, the granodiorite was metamorphosed and deformed. Epidote and chlorite found in the sample suggests metamorphism to greenschist facies. Microstructures in the samples seem to support low temperature metamorphism.

Fracturing of plagioclase, microcline and quartz as the predominate method of deformation typically occurs at greenschist facies metamorphism (Gapais, 1989). Cataclasis is usually accompanied by the development of undulose extinction and deformation banding in quartz at $280 \pm 30^{\circ}\text{C}$ (Pryer, 1993). Undulose extinction in quartz occurs at a higher temperature range, between 400 and 500°C (Passchier and Trouw, 2005).

With increasing temperature, grain boundary migration becomes the dominate method of deformation (Stipp *et al.*, 2002). Grain boundary migration (GBM) includes low temperature pressure solution/bulging, sub-grain formation and rotation. Pressure solution develops along high strain regions along grain boundaries (Pryer, 1993). Fluid along the grain boundaries facilitates dissolution and grain boundary migration (Passchier and Trouw, 2005).

Sub-grain formation and rotation lead to the development of core-and-mantle structures in quartz- feldspathic minerals (Stipp *et al.*, 2002). According to Passchier and Trouw, 2005, core-and-mantle structures in feldspar develop at temperatures above 450°C . Core-and-mantle structures were not found in the granodiorite. This may indicate that maximum metamorphic temperatures did not exceed 450°C .

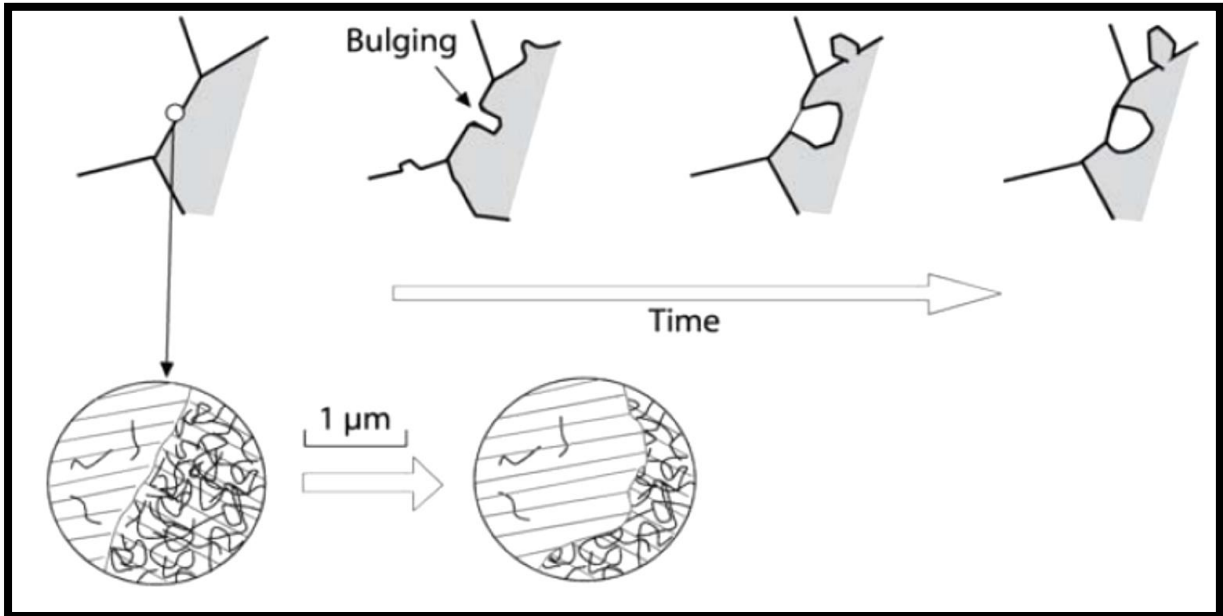


Fig 7.4.1. The adjacent grains have different dislocation concentration. The grain with the lowest dislocation concentration will migrate towards the grain with higher dislocation density. The bulge will eventually pinch off and form a strain-free grain (Passchier and Trouw, 2005).

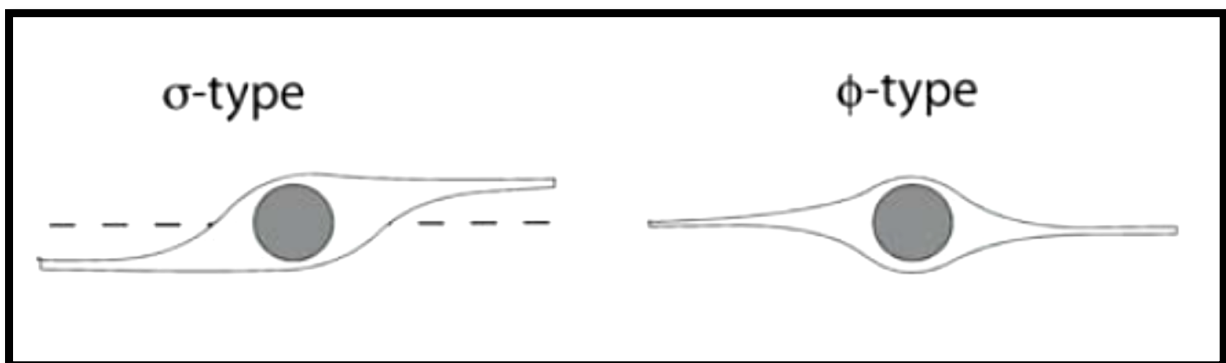


Fig 7.4.2. The centre of the mineral is referred to as the core, surrounded by mantle. The mantle develops from either sub-grain formation that is concentrated on the grain boundaries of ductile deformation of the mineral (Passchier and Trouw, 2005).

7.5. Comparison other regions in the craton similar to the study area

Granitoid intrusion associated with orthogneiss and migmatites were previously described by Hirdes *et al.*, 1996, Doumbia *et al.*, 1998, Gasquet *et al.*, 2003, Naba *et al.*, 2004 and Vegas *et al.*, 2008. The Pissila batholith and the Saaba zone gneiss are petrologically and geochemically similar to gneissic terranes in the sodic calc-alkaline granitoids in the Dabakala region, Côte d'Ivoire and the batholiths in north eastern Burkina Faso (appendix 1). Therefore, the Pissila batholith and the Saaba zone were possibly derived from similar processes that formed the above regions. In both regions the granitoids are associated with first group of granitoid intrusion ca 2.1 Ga, which is similar to the age (2143 ± 12 Ma and 2117 ± 17 Ma) of the Pissila batholith (Gasquet *et al.*, 2003, Vegas *et al.*, 2008).

In a study of granitoid-gneissic terrane in the Dabakala region, Hirdes *et al.*, 1996 proposed that the gneisses were intruded by younger batholiths. The intrusion leads to partial melting and subsequent migmatitisation of the gneisses (Naba *et al.*, 2003). Geochronology of the gneiss produced age ca 2.3 Ga (Gasquet *et al.*, 2003). The gneiss and batholiths are cross-cut by alkaline granites (Vegas *et al.*, 2008). The alkaline granites are associated with second generation pluton that intruded into the batholiths (Doumbia *et al.*, 1998).

Despite the petrological and geochemical similarities with other granitoid-gneissic terranes in the craton, rocks from the study area exhibit some variation. The alkaline granites are pegmatoidal and biotite bearing (Vegas *et al.*, 2008). The alkaline granites (K-rich vein) in the study Saaba zone gneiss are fine-grained and contain little to no biotite. The alkaline granite/K-rich vein exhibit a REE pattern similar to the gneiss. The REE pattern may suggest the alkaline granite/K-rich vein were derived from a source similar to the gneiss and not from an intrusion unrelated to the gneiss.

8. Conclusion

Petrology and geochemistry suggests the Pissila batholith and the Saaba zone gneiss are differ from each other. The gneisses exhibit some affiliations to Archean TTG. The Pissila batholith does not vary too much from other calc-alkaline intrusions in the craton. Geochronology of the batholith produces age of 2143 ± 12 Ma and 2117 ± 17 Ma. Emplacement was coeval with the Eburnean orogeny ca 2.1 Ga.

The Pissila batholith and the Saaba zone exhibit some similarities to granitoid-gneissic terranes in Côte d'Ivoire, NE Burkina Faso and Senegal. The study area may have formed under processes similar to those that formed granitoid-gneisses in the above countries. Therefore, the Saaba zone was possibly intruded by the Pissila batholith. The intrusion leads to partial melting and migmatization of the gneisses.

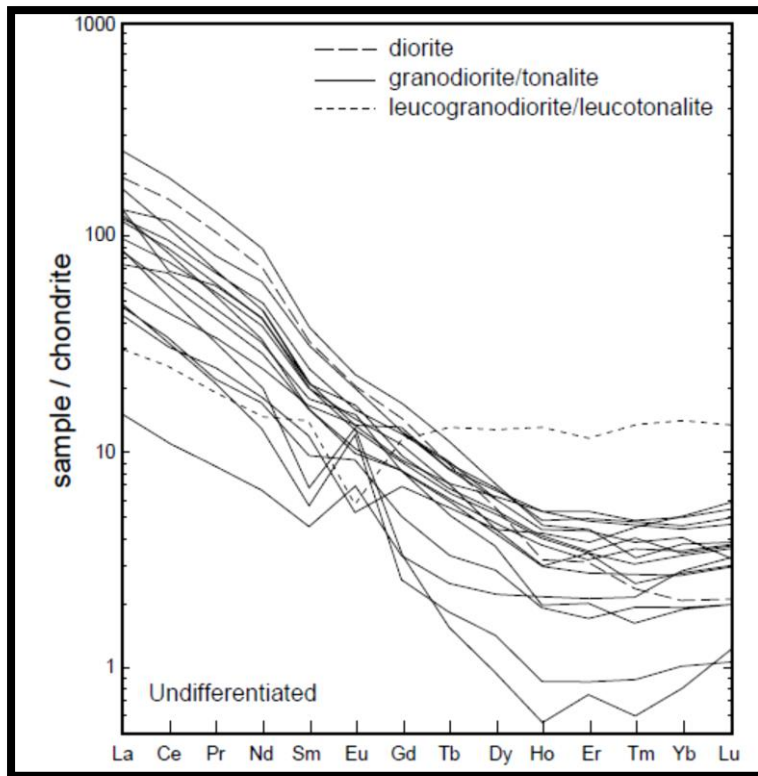
Analysis of microstructures in the Pissila batholith and the Saaba zone gneiss suggests the rocks were subjected to two deformation events. The Saaba zone gneiss and migmatites was deformed to amphibolites facies during D1 deformation event. D2 lead to greenschist facies metamorphism of both the Pissila batholith and the Saaba zone.

Despite petrography and geochemistry indicating that the Pissila batholith and the Saaba zone gneiss are unrelated, more conclusive data is required. Therefore, geochronology of the Saaba zone is necessary to validate the study results. Geochronology would also allow for better comparison of the study area to other granitoid-gneissic terranes in the craton.

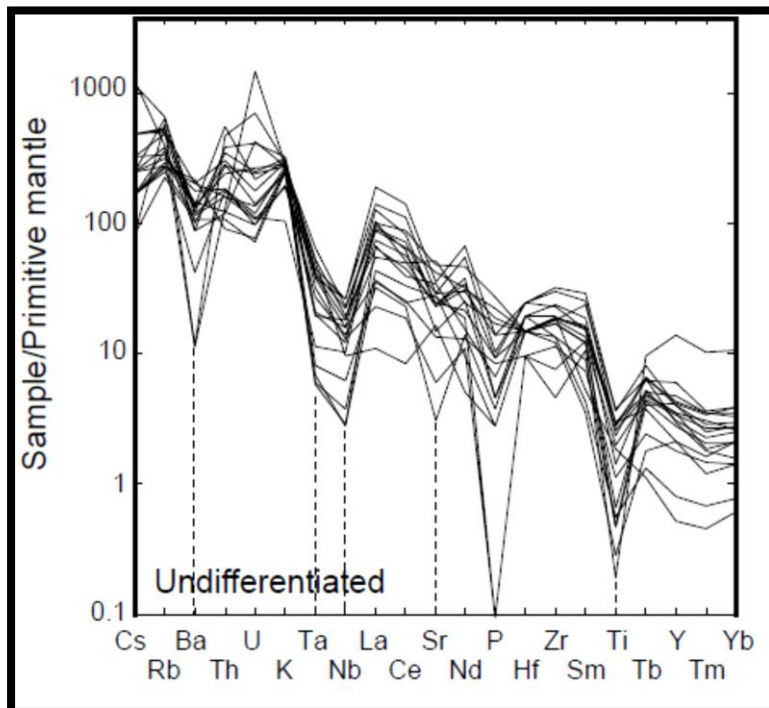
9. *Acknowledgment*

The author would like to thank Profs. Ncube-Hein and Saalman for their supervision, the West African Exploration Initiative (WAXI) group for sponsoring the project and the Earth Lab staff in the University of the Witwatersrand.

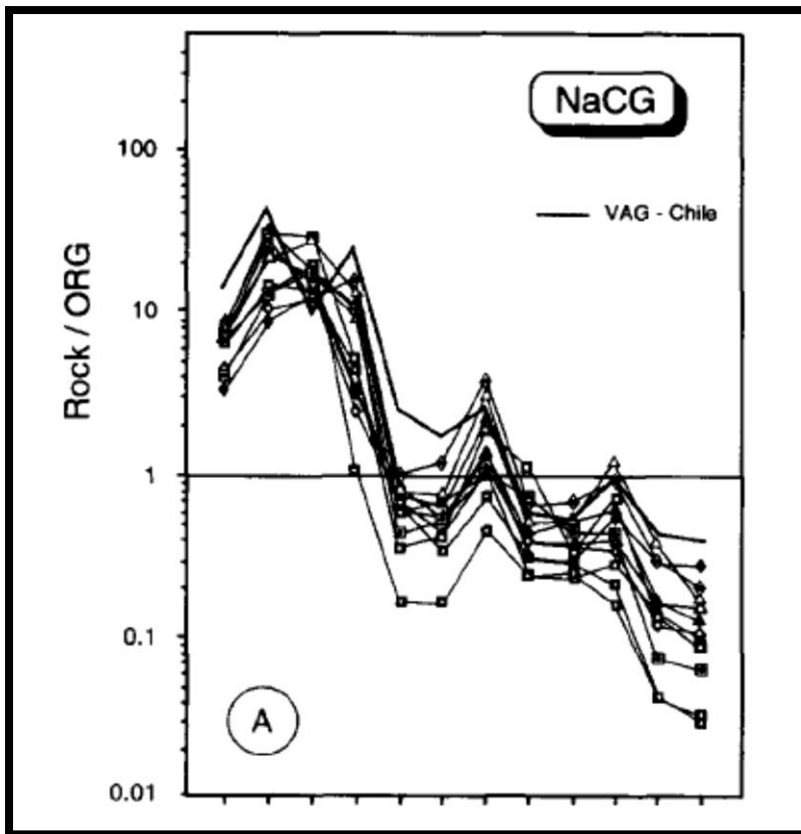
Appendix 1



REE diagrams of the Dabakala region in Côte d'Ivoire (Gasquet *et al.*, 2003)



Spider diagram of the Dabakala region in Côte d'Ivoire (Gasquet *et al.*, 2003)



Spider diagram of the sodic calc alkaline gneiss (Dombia et al., 1998)

REFERENCES;

- Agbossoumonde, Y., Ménot, R.P., Guillot, S., Yéssoufou, C. P., 2007. Petrological and geochronological constraints on the origin of the Palimé-Amlame granitoids (South Togo, West Africa): A segment of the West African Craton Palaeoproterozoic margin reactivated during the Pan African collision. *Gondwana Research* 12, 476-488.
- Baratoux, L., Metelka, V., Naba, S., Jessell, M. W., Grégoire, M., Ganne, J., (2011). Juvenile Paleoproterozoic crust evolution during the Eburnean orogeny (\sim 2.2-2.0 Ga), western Burkina Faso. *Precambrian Research* 191, 18-45.
- Béziat, D., Dubois, M., Debat, P., Nikiéma, S., Salvi, S., Tollon, F. (2008). Gold metallogeny in the Birimian craton of Burkina Faso (West Africa). *Journal of African Earth Science* 50, 215-233.
- Cahen, L., Snelling, N. J., Delhal, J., Vali, J. R., (1984). The geochronology and evolution of Africa. Clarendon Press, Oxford,
- Cairncross, B. (2004). *Field Guide to Rocks and Minerals of Southern Africa*. Struik Publishers, Cape Town 243-245.
- Davis, G. H., Reynolds, S. J. (1996). *Structural Geology of Rocks and Regions* (2nd edition). John Wiley and Sons Inc, Canada, 150-203.
- Debat, P., Nikiéma, S., Mercer, A., Lompo, M., Béziat, D., Bourges, F., Roddaz, M., Salvi, S., Tollen, F., Wenmenga, U., (2003). A new metamorphic constraint for the Eburnean orogeny from Palaeoproterozoic formations of the Man shield (Aribinda and Tampilga countries, Burkina Faso). *Precambrian Research* 123, 47-65.
- Dioh, E., Bézait, D., Debat, P., Cregoire, M., Ngom, P. M., (2006). Diversity of the Palaeoproterozoic granitoids of the Kedougou Inlier (eastern Senegal); Petrographical and geochemical constraints. *Journal of African Earth Science* 44, 351-371.
- Doumbia, S., Pouclet, A., Kouamelan, A., Peucat, J.J., Vidal, M., Delor. (1998). Petrogenesis of juvenile-type Birimian (Paleoproterozoic) granitoids in Central Côte d'Ivoire, West Africa: geochemistry and geochronology. *Precambrian Research* 87, 33-63.
- Egal, E., Thiélbemont, D., Lahondère, D., Guerrot, C., Costea, A. C., Goujou, J. G., Lafon, J. M., Tegye, S. D., Delor, C., Goujou, J. G., Kolié, P. (2002). Late eburnean granitization and tectonics along the western and northern margin of the Archean Kénéman-Man domain (Guinea, West Africa). *Precambrian Research* 117, 57-84.

- Eisenlohr, B. N., Hirdes, W., (1992). The structural development of the early Proterozoic Birimian & Tarkwaian rocks of southwest Ghana, West Africa. *Journal of African Earth Science* 14(3), 313-325.
- Evansen, N. M., Hamilton, P. J., O’Nions R. (1978). Rare-earth abundance in chondritic meteorites, *Geochemica et Cosmochimica Acta* vol 42. Pergamon Press Ltd, Great Britain, 1199-1212.
- Feybesse, J. L., Milési, J.P., (1994). The Archean/ Proterozoic contact zone in West Africa: a mountain belt of décollement thrusting and folding on a continental margin related to 2.1 Ga convergence of Archean craton? *Precambrian Research* 69,199-227.
- Feybesse, J. L., Billa, M., Guerrot, C., Duguey, J. L. L., Milési, J. P., Bouchot, V., (2006). The paleoproterozoic Ghanian province: Geodynamic model and ore controls, including regional stress modelling. *Precambrian Research* 149, 149-196.
- Gapais, D. (1989). Shear structures within deformed granites: Mechanical and thermal indicators. *Geology* 17: 114-1147.
- Gasquet, D., Barbey, P., Adou, M., Paquette, J.L., (2003). Structure Sr-Nd isotope geochemistry and zircon U-Pb geochronology of the granitoids of the Dabakala area (Côte d’Ivoire): evidence for a 2.5 Ga crustal growth event in the Palaeoproterozoic of West Africa. *Precambrian Research* 127, 320-354.
- Hasting, D. A., (1982). On the tectonics and metallogenesis of West Africa: A model incorporating new geophysical data. *Geoexploration* 20, 295-327.
- Hein, K. A. A., Morel, V., Kagoné, O., Kiemde, F., (2004). Birimian lithological succession and structural evolution in the Gorem segment of the Boromo-Goren Greenstone Belt, Burkina Faso. *Journal of African Earth Science* 39, 1-23.
- Hirdes, W., Davis, D.W., Lüdte, G., Konan, G. (1996). Two generations of Birimian (Paleoproterozoic) volcanic belts in northeastern Côte d’Ivoire (West Africa): *Precambrian Research* 80, 173-191.
- Holland, H. D. and Turekian K. K. (2003). *Treatise of Geochemistry* volume 1. Elsevier Pergamon, New York , 358-397, 517-521.
- Kouamelan, A. N., Delor, C., Peucat, J.J., (1997). Geochronological evidence for reworking of Archean terrain during the Early Proterozoic (2.1 Ga) in the western Côte d’Ivoire (Man Rise-West African Craton) *Precambrian Research* 86, 177-199.
- Kruhl, J.H. (1996). Prism- and Basal- plane parallel subgrain boundaries in quartz: a microstructural geothermobarometer. *Journal of metamorphic geology* 14, 581-589.

- Martin, H., Smithies, R. H., Rapp, R., Moyen, J. F., Champion D. (2005). An overview of adakite, tonalite-trondhjemite-granodiorite (TTG) and sanukitoids: relationships and some implications for crustal evolution. *Lithos* 79, 1-24.
- Martin, H. And Moyen, J. F. (2002). Secular changes in tonalite-trondhjemite-granodiorite composition as a marker of progressive cooling of the Earth. *Geology* 30, 319-322.
- Martin, H., Moyen, J. F., Rapp, R. (2010). The sanukitoid series: magmatism at the Archean-Proterozoic transition. *Earth and Environmental Science Transaction of the Royal Society of Edinburgh* 100, 15-33.
- Milési, J.P., Ledru, P., Feybesse, J.L., Dommangeat, A., Marcoux, E., 1992. Early Proterozoic ore deposits and tectonics of the Birimian orogenic belt, West Africa. *Precambrian Research* 58, 305-344.
- Naba, S., Lompo, M., Debat, P., Bouchez, J. L., Bézait, D., (2004). Structure and emplacement model for late orogenic Palaeoproterozoic granitoids: the Tenkodogo-Yamba elongation pluton (Eastern Burkina Faso). *Journal of African Earth Science* 38, 41-57.
- Passchier, C. W., Trouw, R. A. J., (2005). *Microtectonic* (2nd edition). Springer-Verlag, Berlin.
- Pohl, D., (1998). A decade of change-mineral exploration in West Africa. *The Journal of the South African Institute of Mining and Metallurgy*, 311-316.
- Pons, J., Barbey, P., Dupus, D., Leger, J. M. (1995). Mechanisms of pluton emplacement and structural evolution of a 2.1 Ga Juvenile continental crust: Birimian of south western Niger. *Precambrian Research* , 70, 281-301.
- Potrel, A., Fanning, C. M., (1998). Archean crustal evolution of the West African Craton: example of the Amsaga Area (Reguibat Rise). U-Pb and Sm-Nd evidence for crustal growth and recycling. *Precambrian Research* 90, 107-117.
- Pryer, L.L. (1993). Microstructures in feldspar from a major crustal thrust zone: Grenville Front, Ontario, Canada. *Journal of Structural Geology* 15(1), 21-36.
- Roddaz, M., Debat, P., Nikiéma, S. (2007). Geochemistry of Upper Birimian sediments (major and trace elements and Nd-Sr isotopes) and implications for weathering and tectonic setting of the Late Paleoproterozoic crust. *Precambrian Research* 159, 197-211.
- Rollinson, H. (1993). *Using geochemistry data: evaluation, presentation, interpretation*. Longman Scientific and Technical, New York, 48-170.
- Sawyer, W. (2008). *Atlas of migmatites*. NRC-Research Press, Canada, 1-47.

- Skinner, E., Apter, D.B., Marcelli, C., Smithson, N.K., (2004). Kimberlites of the Man Craton, West Africa. *Lithos* 76, 233-259.
- Smithies, R. H. (2000). The Archean tonalite-trondhjemite-granodiorite (TTG) series is not analogue of Cenozoic adakites. *Earth and Planetary Science Letter* 182, 115-125.
- Stripp, M., Stunitz H., Heilbronner, R., Schmid, S. M. (2002). The eastern Tonale fault zone: a natural laboratory for crystal plastic deformation of quartz over a temperature range from 250 to 700°C. *Journal of Structural Geology* 24, 1861-1884.
- Sun, S. (1982). Chemical composition and origin of the earth's primitive mantle. *Geochemica et Cosmochimica Acta* vol 46. Peragamon Press Ltd, Great Britain, 179-192.
- Thielbement, D., Goujou, J.C., Egal, E., Cochene, A., Delor, C., Lafon, J.M., Fanning, C.M., (2004). Archean evolution of the Leo-Rise and its Eburnean reworking. *Journal of African Earth Science* 39, 97-104.
- Thompson, R. N. (1982). Magmatism of the British Tertiary Volcanic Province. *Scottish Journal of Geology* 18, 49-107.
- Tshibubudze, A., Hein, K. A. A., Marquis, P., (2009). The Markoye Shear in NE Burkina Faso. *Journal of African Earth Science* 55, 245-256.
- Vegas, N., Naba, S., Bouchez J.L., Jessel, M. (2008). Structural and emplacement of granites in the Palaeoproterozoic crust of Eastern Burkina Faso: rheological implications. *International Journal of Earth Science (Geology Rundsch)* 97, 1165-1180.
- White, W. M. (2012). *Geochemistry*. Wiley and Blackwell, New York, 258-306, 512-549.

SPONSORS



WAXI- West African Exploration Initiative
IXOA- L'Initiative d'Exploration Ouest Africaine

Project Broker & Coordinator



Research Partners












Sponsor: Capacity Building



Australian Government
AusAID

Sponsors in kind (Geological Surveys)

 Liberia	 Mali	 Niger
 Mauritania	 Guinea	 Burkina Faso
 Senegal	 Ghana	 Togo

Sponsors: Research Program







































43